

## Disulfide bridge formation influences ligand recognition by the ATAD2 bromodomain

Jamie C. Gay<sup>1</sup>, Brian E. Eckenroth<sup>2</sup>, Chiara M. Evans<sup>1</sup>, Cassiano Langini<sup>3</sup>, Samuel Carlson<sup>1</sup>, Jonathan T. Lloyd<sup>1</sup>

Amedeo Caflisch<sup>3</sup> and Karen C. Glass<sup>1\*</sup>

<sup>1</sup>From the Department of Pharmaceutical Sciences, Albany College of Pharmacy and Health Sciences,  
Colchester, VT, 05446, USA

<sup>2</sup>Department of Microbiology and Molecular Genetics, University of Vermont, Burlington, VT 05405, USA

<sup>3</sup>From the Department of Biochemistry, University of Zurich, CH-8057 Zurich, Switzerland

Running title: *Disulfide bridge formation in the ATAD2 bromodomain*

\*To whom correspondence should be addressed: Karen C. Glass, Department of Pharmaceutical Science,  
Albany College of Pharmacy and Health Sciences, 261 Mountain View Dr., Colchester, VT 05446, USA, Tel.:  
802-735-2636; Fax: 802-654-0716; E-mail: karen.glass@acphs.edu

### SUPPLEMENTARY DATA

**Supplementary Figure S1. Codon optimization of the ATAD2 bromodomain sequence.** The DNA sequence of the codon optimized human ATAD2 bromodomain for expression in *Escherichia coli*.

```
CAAGAAGAAGACACATTCCGCGAACTGCGCATATTTCTCCGCAACGTAACACATCGCTTGGCTAT
AGACAAAAGATTTAGAGTTTTCACTAAACCGGTAGACCCGGACGAAGTACCGGACTACGTCACCG
TAATAAAACAACCGATGGACTTGTCTAGCGTAATCTCTAAGATAGACCTACATAAATACCTGACTG
TTAAGGACTACTTGCGCGACATAGACCTAATCTGTTCTAACGCACTCGAATACAACCCGGACCGC
GACCCGGGAGACCGATTGATACGCCATCGCGCATGTGCTCTCCGCGACACTGCATACGCAATAAT
AAAGGAAGAATTGGACGAAGACTTCGAACAGCTCTGTGAAGAAATACAGGAAAGCCGC
```

**Supplementary Figure S2. Isomorphous and anomalous difference maps corresponding to sulfur atoms**

**in the ATAD2 bromodomain structure.** A. Shown is the Fo-Fo isomorphous difference Fourier map calculated using Phenix<sup>1</sup> between 3DAI<sup>2</sup> (red) and 6CPS (green) contoured at 3 sigma. The R-factor between the two data sets was determined to be 31.4% for F(obs) as calculated using CAD and Scaleit within CCP4<sup>3</sup> indicating significant differences between the two structures. Structural perturbations were clearly observed in the isomorphous difference maps, including partial formation of a disulfide bond. The HEPES is also observed in the difference map though its clarity is influenced by the water molecules bound in 3DAI. B. and C. Shown are the anomalous difference Fourier maps for 3DAI (cyan) and 6CPS (yellow-orange). Anomalous maps were calculated using Phenix with data to 4 angstroms as estimated for the limit of anomalous signal using Xtriage<sup>1</sup>. Maps were contoured to 3 sigma and showed equivalent peak heights for the anomalous scattering sulfurs from M1029, C1101 and two sulfates bound from the crystallization conditions. Significant difference was observed for the C1057 and C1079.

**Supplementary Figure S3. Measurement of the ATAD2 bromodomain binding activity by ITC. (A)**

Exothermic ITC enthalpy plot for the binding of the wild-type, non-codon-optimized ATAD2 (WT ATAD2) bromodomain and the histone H4K5ac peptide ligand (res 1-10). (B-D) Exothermic ITC enthalpy plots comparing binding of the ATAD2 triple cysteine bromodomain mutant with no disulfide bridge to the ATAD2 bromodomains with either 49% or 100% disulfide bridge formation to the histone H4K5ac peptide ligand (res 1-10). (E-G) Exothermic ITC enthalpy plots comparing binding of the ATAD2 triple cysteine bromodomain mutant with no disulfide bridge to the ATAD2 bromodomains with either 49% or 100% disulfide bridge formation to the binding of GSK compound 38<sup>51</sup>.

**Supplementary Figure S4. The sulfur atoms are in van der Waals contact.** Time trace of the distance between the sulfur atoms of C1057 and C1059. When the disulfide bridge is formed (slate line and dots) the distance is restrained by the covalent bond. The average distance for the trajectory without the disulfide bridge (orange line and dots) is 4.61 Å, which provides evidence that the two sulfur atoms are most of the time in

optimal van der Waals contact. The dots represent all data points and the solid line is a moving average with a window of 100 data points.

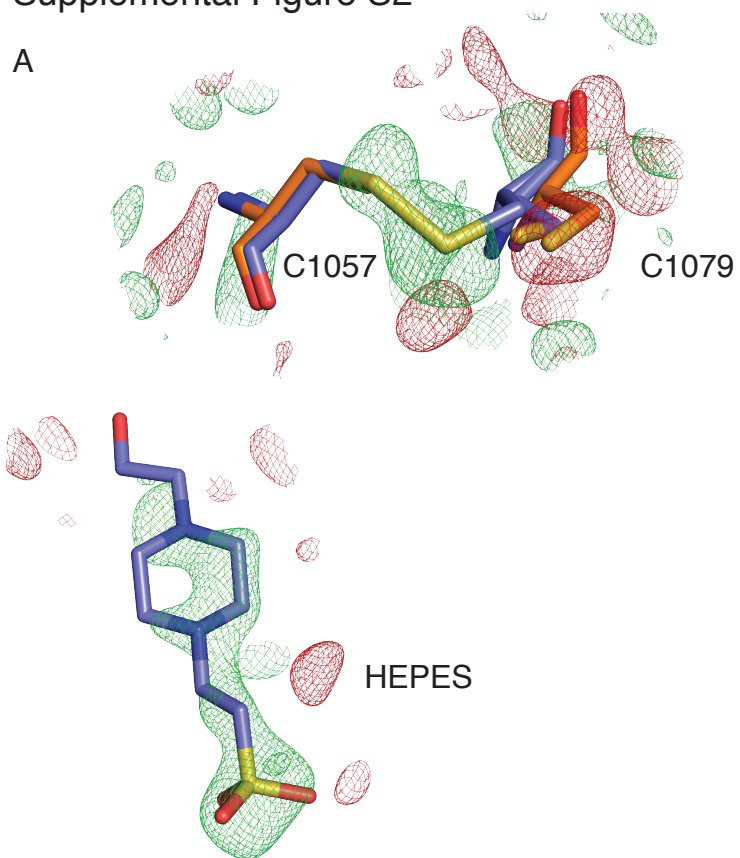
**Supplementary Figure S5. Rotameric states of I1074 and V1008.** 2D histogram density estimates of the  $\chi_2$  angle of I1074 (gatekeeper residue) versus the  $\chi_1$  angle of V1008 (part of the 'RVF' shelf). The plot overlays data from the simulation with (slate) and without (orange) the disulfide bridge formed.

#### References:

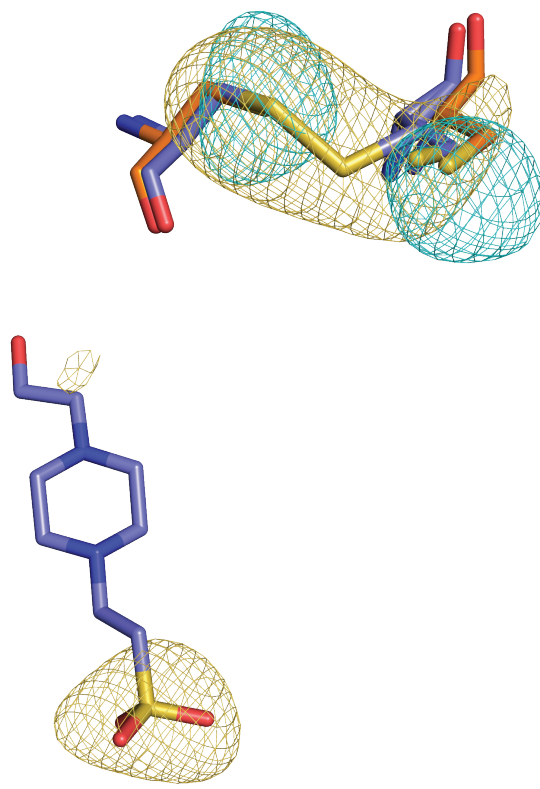
1. Adams PD, Afonine PV, Bunkoczi G, Chen VB, Davis IW, Echols N, Headd JJ, Hung LW, Kapral GJ, Grosse-Kunstleve RW, McCoy AJ, Moriarty NW, Oeffner R, Read RJ, Richardson DC, Richardson JS, Terwilliger TC, Zwart PH. PHENIX: a comprehensive Python-based system for macromolecular structure solution. *Acta Crystallogr D Biol Crystallogr* 2010;66(Pt 2):213-221.
2. Filippakopoulos P, Picaud S, Mangos M, Keates T, Lambert JP, Barsyte-Lovejoy D, Felletar I, Volkmer R, Muller S, Pawson T, Gingras AC, Arrowsmith CH, Knapp S. Histone recognition and large-scale structural analysis of the human bromodomain family. *Cell* 2012;149(1):214-231.
3. COLLABORATIVE COMPUTATIONAL PROJECT N. The CCP4 Suite: Programs for Protein Crystallography. *Acta Cryst* 1994;D50:760-763.

# Supplemental Figure S2

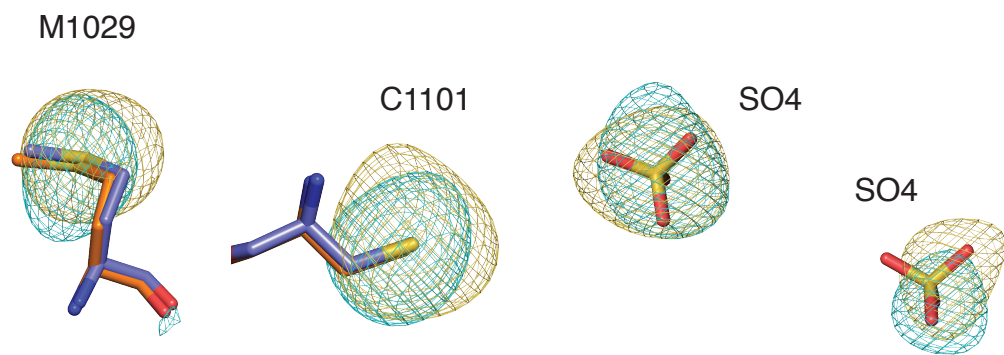
A



B

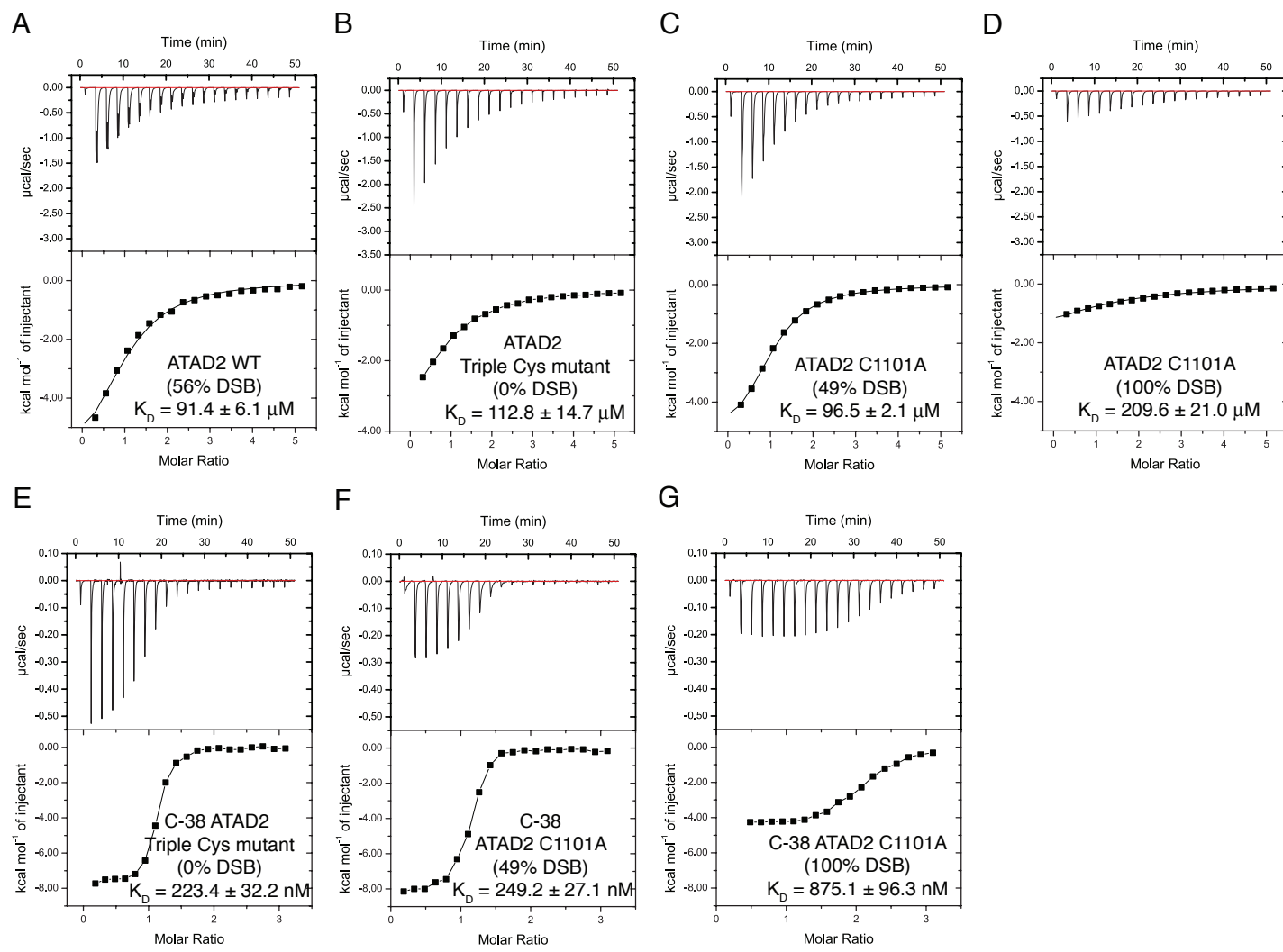


C

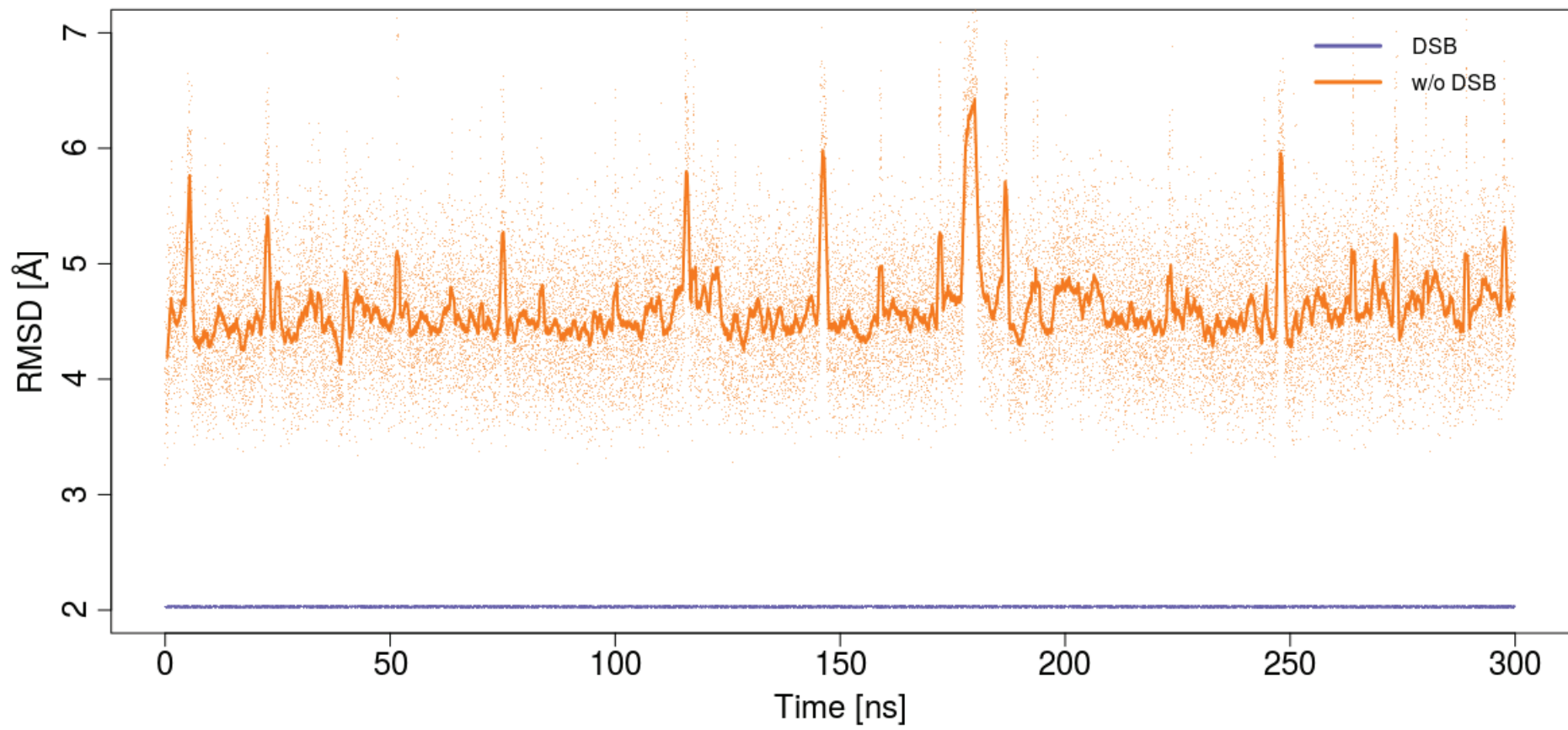




Supplemental Figure S2



Supplemental Figure S4



Supplemental Figure S5

